

# Synthesis, crystal growth and characterization of new semi-organic nonlinear optical material- L-proline barium nitrate (LPBN)

P. MOHAMED KUTTY<sup>a</sup>, J. CHANDRASEKARAN<sup>b,\*</sup>, B. BABU<sup>b,c</sup>, A. NIZARUL HAZEEN<sup>a</sup>

<sup>a</sup>Research and Development Center, Bharathiar University, Coimbatore - 641 046, Tamil Nadu, India

<sup>b</sup>Department of Physics, Sri Ramakrishna Mission Vidyalaya College of Arts and Science, Coimbatore – 641 020, Tamil Nadu, India

<sup>c</sup>Department of Science and Humanities, Sri Krishna College of Engineering and Technology, Coimbatore-641 008, Tamil Nadu, India

A new semi-organic crystal L-proline barium nitrate (LPBN) was grown by slow evaporation solution growth technique at room temperature. The crystal structure was confirmed by the single crystal XRD analysis. Powder XRD analysis confirms the crystalline nature of the compound. Various functional groups present in the compound were confirmed through the FTIR analysis. UV studies shows that the crystal is transparent in the entire visible region. Microhardness studies reveal the soft nature of the grown crystal. TG-DTA studies shows that LPBN is stable up to 270°C. A powder second harmonic generation study confirms the SHG conversion efficiency of L-proline barium nitrate is 1.77 times greater than that of standard KDP.

(Received December 8, 2014; accepted February 10, 2016)

**Keywords:** Crystal growth, Nonlinear, X- ray diffraction, Powder SHG

## 1. Introduction

In recent years nonlinear optical (NLO) materials have gained a great attention in optical devices like optical switches, optical modulators, optical logic, optical data storage, electro-optical devices, optical parametric oscillation, optical bistability and laser remote sensing etc [1-3]. In this regard a number of organic and inorganic materials have already been studied [4]. Predicting more efficient nonlinear materials with desirable properties is one of the main challenges in the field of nonlinear optics. Organic NLO materials offer many advantages over inorganic NLO materials. Organic materials are formed by weak Van der Waals and hydrogen bonds, hence they possess a high degree of delocalization, inherent ultrafast response time, electronic susceptibility ( $\chi^{(2)}$ ), molecular polarizability ( $\beta$ ), high laser damage threshold, ease of device fabrication and flexibility of molecular design via proper synthetic method. But they possess very poor thermal and chemical stability and it is difficult to grow large size crystals. Their mechanical property also is very low when compared to inorganic materials. Inorganic materials possess very low nonlinearity. Hence new types of hybrid organic-inorganic NLO materials were grown with the high optical non-linearity of purely organic compounds combined with the excellent mechanical and thermal properties of inorganic materials [5-8]. These semi-organic nonlinear materials gain the advantages of both inorganic and organic properties.

L-proline is an  $\alpha$ -amino acid, one of the twenty DNA coded amino acids. It forms a number of complexes in reaction with inorganic acids and salts to produce an outstanding material for NLO applications. Also it is the

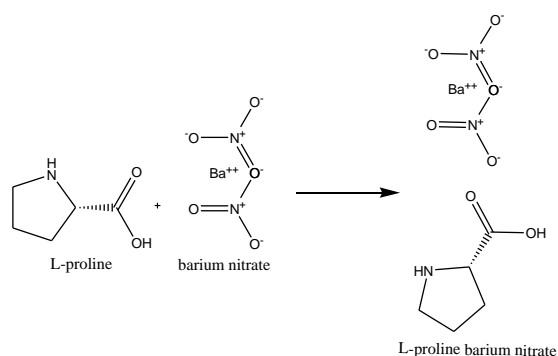
only one which contains an imino group (-NH) instead of an amino (NH<sub>2</sub>) group and as widely used as a laser frequency doubler and electro optic modulator. A series of studies on L-proline based semi-organic compounds such as Bis L-proline hydrogen nitrate, L-proline dimercuric chloride, L-Proline trichloroacetate, L-proline strontium chloride monohydrate, Dibromobis(L-proline) Zinc (II), L-proline lithium chloride monohydrate, L-Proline Cadmium Chloride Monohydrate were studied and their nonlinear properties were reported [9-16]. In this paper semi-organic crystal of L-proline barium nitrate was grown from slow evaporation solution growth technique. The grown crystals were characterized by various characterization techniques such as single crystal XRD, powder XRD, FT-IR, UV, TG-DTA, microhardness, EDX and powder SHG studies.

## 2. Experimental

### 2.1. Crystal growth

In the present work, LPBN crystals were grown from slow evaporation solution growth technique at room temperature. Commercially available high purity L-proline (C<sub>5</sub>H<sub>9</sub>NO<sub>2</sub>) (Himedia, 98%) and barium nitrate (E-Merck, 98%) were taken in the molar ratio of 1:1 and dissolved in triple distilled water and the solution was thoroughly stirred for 3 hrs at 50°C using a magnetic stirrer to yield a homogeneous mixture solution. Then the homogeneous solution was filtered using whatmann filter paper (No.42) and transferred into a crystallizing vessel. In order to control the evaporation rate, the top of the beaker was

covered with a thin plastic sheet and the content was subjected to the slow evaporation process at room temperature. After two weeks good quality crystals were harvested from the mother solution. Reaction scheme is depicted in scheme 1. The quality of the as grown crystal is depicted in Fig. 1.



Scheme 1. Reaction scheme of LPBN.



Fig. 1. As grown crystal of LPBN.

### 3. Results and discussion

#### 3.1. X-ray diffraction analysis

The grown single crystals of the LPBN was subjected to single crystal XRD studies using a ENRAF NONIUS CAD-4 X-Ray diffractometer with MoK $\alpha$  ( $\lambda=0.7107$  Å). The data was collected at room temperature. We found that the grown LPBN crystals belong to the orthorhombic system with the noncentrosymmetric space group P2<sub>1</sub>2<sub>1</sub>2<sub>1</sub>. The observed lattice dimensions are  $a=7.1405$  (5)Å,  $b=13.469$  (1)Å,  $c=19.7670$  (16)Å and volume=1901.10Å<sup>3</sup>. In order to study the crystalline nature of the sample the grown single crystals of LPBN were finely crushed into powder using an agate mortar and subjected to the powder XRD analysis. The sample was scanned over the  $2\theta$  range of 10-80° at a rate of 3° per/min. The indexed powder XRD pattern is shown in Fig. 2. A maximum intensity of 30782 counts was observed for the title compound. The appearance of quite sharp diffraction peaks shows that the LPBN crystal is free from structural grain boundaries and the crystalline nature is good [17].

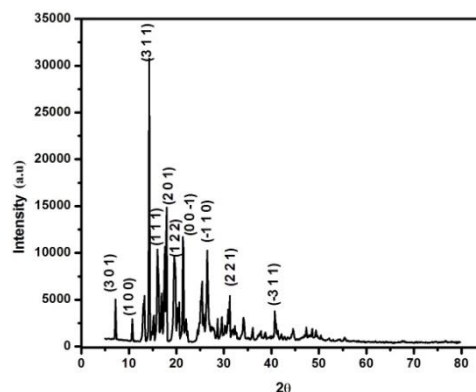


Fig. 2. Powder XRD spectrum of LPBN.

#### 3.2. FTIR studies

The Middle infrared (FTIR) spectrum of the LPBN were recorded at room temperature in the range of 4000 to 400 cm<sup>-1</sup> using a Bruker FTIR 4100 spectrometer by a standard KBr pellet method. The recorded spectrum is shown in Fig. 3. In the spectrum vibration at 3433 cm<sup>-1</sup> is assigned to both N-H and OH stretching vibrations. The symmetric stretching vibration of COO<sup>-</sup> appears at 1416 cm<sup>-1</sup>. Also this vibration is assigned to CH<sub>2</sub> bending. The aromatic C-H stretching vibration appears at 2743 and 2813 cm<sup>-1</sup>. Ring skeletal deformation takes place at 727 cm<sup>-1</sup>. C=O stretching vibration was observed at 2468 cm<sup>-1</sup>. Vibrations at 1776 and 1380 cm<sup>-1</sup> are assigned for COO<sup>-</sup> and C-O bond stretching frequency. C-H bending vibration occurred at 1380 cm<sup>-1</sup>. The rocking mode of CH<sub>2</sub> observed at 814 cm<sup>-1</sup>.

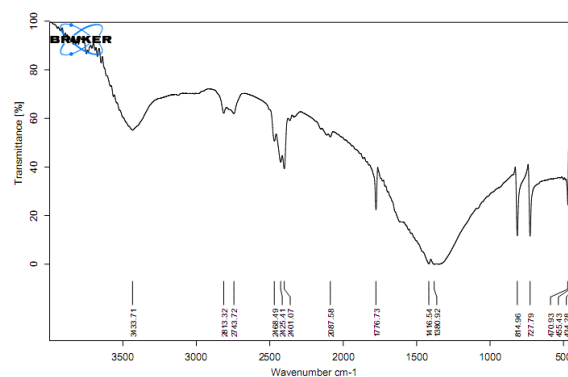


Fig. 3. FTIR spectrum of LPBN crystal.

#### 3.3 UV-Vis spectral analysis

The optical transmittance and absorption spectrum of the LPBN was recorded in the wavelength of 200-1100 nm covering the near UV, Visible and NIR region by using the Jasco UV-Vis spectrophotometer at room temperature. For optical device applications the crystal could be transparent in the considerable wavelength region. The recorded transmittance spectrum is shown in Fig. 4, which indicates

that the crystal has transmittance in the entire visible region and there is no significant absorption between 328 nm and 1100 nm. The optical band gap was evaluated by extrapolating the linear portion of  $h\nu$  vs  $(\alpha h\nu)^{1/2}$ . The estimated optical band gap is about 3.5eV (Fig. 5). The absence of absorption and wide transmittance in the visible region makes the crystal suitable for opto-electronic applications. At lower temperatures the active trapping of impurities by the growing crystal leads to the formation of different defects [18] as a result to the increase the optical absorption or decrease of transmission [19]. The increase in the percentage of optical transmittance in LPBN crystal may be due to the absence of solvent inclusions [20], which in turn reduced scattering centers and increases the output intensity [21]. Also materials with high band gap are expected to possess high laser damage threshold [22].

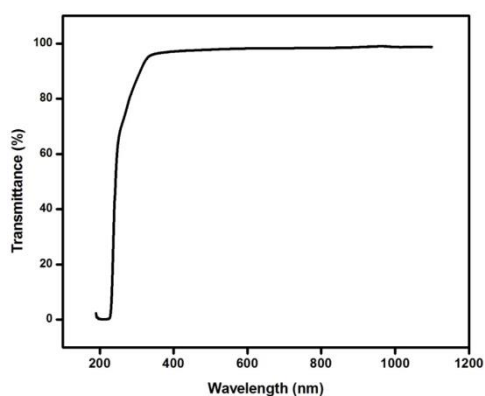


Fig. 4. Optical transmittance spectrum of LPBN.

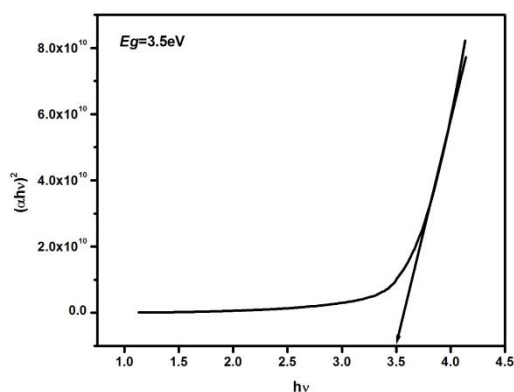


Fig. 5.  $(\alpha h\nu)^2$  vs  $h\nu$ .

### 3.4. TG-DTA analysis

In order to analyze the thermal stability and melting point of the compound, thermo gravimetric (TG) and differential thermal analyses were carried out in the temperature range 30°C to 750°C using the NETZSCH STA 409°C thermal analyzer under nitrogen atmosphere at a heating rate of 10°C/min. Fig. 6 shows the TG-DTA curves of LPBN crystal. From the graph it is observed that the thermal decomposition of the LPBN has taken place in

three stages. In DTA the sharp exothermic peak at 270°C corresponds to the melting point of the crystal. The TG curve indicates that first stage of weight loss occurs at 270°C which very well matches with the DTA. There is no significant weight loss below 270°C, which confirms the absence of water molecules in the molecular structure. The sharpness of the exothermic peak shows the crystallinity and purity of the sample. The TG weight loss at the other two stages is due to the release of volatile substances such as CO<sub>2</sub>, NH<sub>3</sub>, NO<sub>2</sub>, NO, CH<sub>4</sub> etc. Finally the small amount of carbon is present as a residue. It is meaningful to mention that the thermal stability of the LPBN is superior to the other L-proline based semi-organic crystals (Table 1). This ensures the suitability of the LPBN crystals for possible application in the laser where the crystals are required to withstand at high temperature. From the TG-DTA results it can be concluded that the grown the LPBN crystal can be utilized for optoelectronic device applications up to 270°C.

Table 1. Comparison of thermal stability of LPBN.

| Material Name                            | Melting Point [Ref] |
|--|---------------------|
| Bis L-proline hydrogen nitrate           | 235°C [9]           |
| L-Proline trichloroacetate               | 128°C [11]          |
| L-proline strontium chloride monohydrate | 180°C [12]          |
| Dibromo bis(L-proline) Zinc (II)         | 229°C [13]          |
| LPBN present work                        | 270°C               |

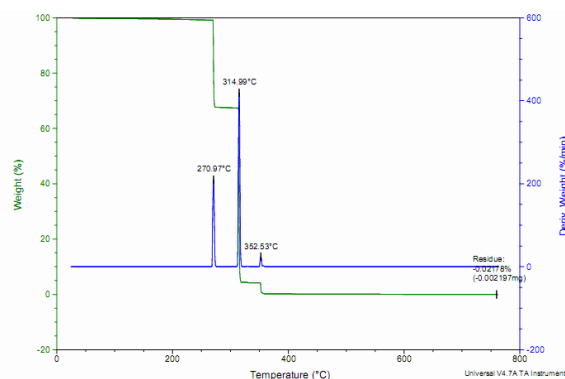


Fig. 6. TG-DTA spectrum of LPBN crystal.

### 3.5 Mechanical studies

Microhardness study is a measure of resistance it offers to local deformation. Microhardness studies for the grown LPBN crystals were carried out using a LEITZ WETZLAR Vickers Microhardness pyramidal indenter attached to an incident light microscope. The grown LPBN crystal was properly mounted on the base of the microscope and the indentations were made on the surface by varying the applied load from 25g to 100g. In the present study measurements were made at room

temperature with a constant indentation time of 15s. Four indentations were made for each load and the average diagonal lengths of the indented impressions were measured using an optical microscope. The Vickers microhardness number was calculated using the given expression

$$H_v = 1.8554 \left( \frac{P}{d^2} \right) (kg/mm)^2$$

where P is the applied load in g and d is the average diagonal length of the indented impression in micro meter. Fig. 7 shows the variation of  $H_v$  as a function of the applied field. It is very clear from the figure that the hardness value increases with increase in load and the crystal exhibits the reverse indentation size effect (RISE). An increase in the mechanical strength will have significant effect on NLO device fabrication and processing such as ease in polishing [23] and less wastage due to cracking / breakage while polishing [24]. On further increase in the load above 100g micro cracks were observed, owing to the release of internal stress generated locally by a deformation. The plot of Log P against Log d gives the value of n and it is determined to be 2.84 (Fig. 8). According to Onitsch and Hanneman n should lie between 1 and 1.6 for harder materials and above 1.6 for softer materials [25]. Hence the grown LPBN crystal belongs to the soft material category.

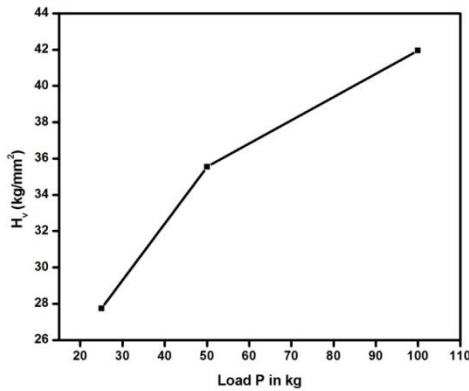


Fig. 7. Plot of Vickers hardness number against load P.

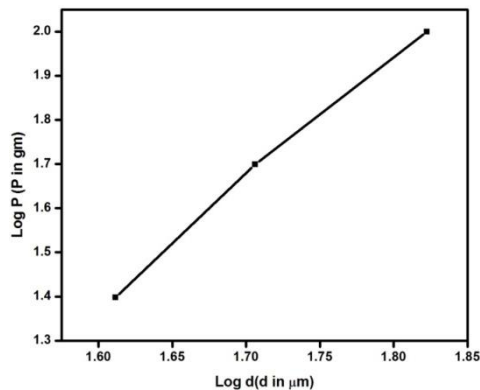


Fig. 8. Log P Vs Log d.

### 3.6 EDX analysis

The elemental composition of the LPBN was investigated by using the energy dispersive analysis. It is the method most commonly used for investigating the elemental composition of the materials. The EDX analysis was carried out using a JEOL model JED-2300 scanning electron microscope. The recorded spectrum is depicted in Fig. 9. It confirms the presence of barium in the title compound.

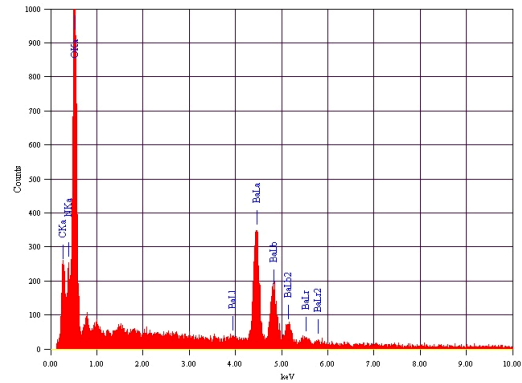


Fig. 9. EDX spectrum of LPBN crystal.

### 3.7. Powder SHG measurement

The PSHG efficiency of the LPBN was tested by using a modified Kurtz and Perry technique [26]. A Q-switched Nd:YAG laser beam of the wavelength of 1064 nm was used for SHG measurements with an input power of 3.5 mJ/pulse. The pulse width was maintained at 8 ns at the repetition rate of 10 Hz/pulse. The grown crystal was ground to a uniform size of about 250 μm particles and packed in a capillary of uniform tube. The SHG behavior of the crystalline material was confirmed from the emission of green radiation (532 nm). The intensity of the green light was measured using a photo multiplier tube and CRO. Powder crystalline KDP was used as the reference material. The SHG conversion efficiency of the LPBN (16mV) is about 1.77 times greater than that of standard KDP (9mV). Powder SHG efficiency of LPBN was compared with other semi-organic crystals and are listed in Table 2.

Table 2. Comparison of SHG efficiency of LPBN.

| Material Name                            | SHG efficiency [Ref] (Reference KDP) |
|--|--------------------------------------|
| L-proline strontium chloride monohydrate | 0.078 [12]                           |
| Dibromo bis(L-proline) Zinc (II)         | 1.5 [13]                             |
| LPBN present work                        | 1.77                                 |

#### 4. Conclusions

A new semi-organic nonlinear optical crystal L-proline barium nitrate was grown from an aqueous solution growth at room temperature. A powder XRD analysis confirms the crystalline nature of the compound. The functional groups present in the compound were confirmed through FT-IR studies. Optical transmittance studies show that the crystal is transparent in the entire visible region. The TG-DTA analysis indicates that the crystal is stable up to 270°C. The powder SHG efficiency is 1.77 times greater than that of standard KDP. The microhardness analysis confirms the soft nature of the crystal.

#### Acknowledgements

The authors gratefully acknowledge the financial support from the DST, Government of India, for the major research project (SB/EMEQ-293/2013).

#### References

- [1] V. Chithambaram, S. Jerome Das, S. Krishnan, J. Alloys Compd. **509**, 4543 (2011).
- [2] V. Ravindrachary, Vincent Crasta, R. F. Bhajantri, Boja Poojari, J. Cryst. Growth **275**, e313 (2005).
- [3] T. Thilak, M. Basheer Ahamed, G. Marudhu, G. Vinitha, Arabian J. Chem. DOI:10.1016/j.arabjc.2013.04.022 (2013).
- [4] B. Babu, J. Chandrasekaran, S. Balaprabhakaran, P. Ilayabarathi, Mater. Sci. Poland **31**, 151 (2013).
- [5] L. Guru Prasad, V. Krishnakumar, R. Nagalakshmi, Physica B **405**, 1652 (2010).
- [6] L. Guru Prasad, V. Krishnakumar, R. Nagalakshmi, Spectrochim. Acta A: Mol. Biomol. Spectrosc. **110**, 377 (2013).
- [7] M. Anbuechezhiyan, S. Ponnusamy, C. Muthamizhchelvan, Physica B **405**, 1119 (2010).
- [8] P. Hemalatha, V. Veeravazhuthi, A. Chandramohan, J. Cryst. Growth **311**, 4317 (2009).
- [9] K. Selvaraju, K. Kirubavathi, Spectrochim. Acta A: Mol. Biomol. Spectrosc. **115**, 537 (2013).
- [10] D. Kalaiselvi, R. Jayavel, Appl. Phys. A **107**, 93 (2012).
- [11] P. Kalaiselvi, S. Alfred Cecil Raj, K. Jagannathan, N. Vijayan, G. Bhagavannarayana, S. Kalainathan, Spectrochim. Acta A: Mol. Biomol. Spectrosc. **132**, 726 (2014).
- [12] Manoj K. Gupta, Nidhi Sinha, Binay Kumar, Physica B **406**, 63 (2011).
- [13] G. Venkatesan, G. Anandha Babu, P. Ramasamy, A. Chandra Mohan, J. Mol. Struct. **1033**, 121 (2013).
- [14] T. Uma Devi, N. Lawrence, R. Ramesh Babu, S. Selvanagayaam, Helen Stoeckli Evans, K. Ramamurthi, Cryst. Growth Des. **9**, 1370 (2009).
- [15] A. Kandasamy, R. Siddeswaran, P. Murugakoothan, P. Suresh Kumar, R. Mohan, Cryst. Growth Des. **7**, 183 (2007).
- [16] Kanika Thukral, N. Vijayan, Brijesh Rathi, G. Bhagavannarayana, Sunil Verma, J. Philip, Anuj Krishna, M. S. Jeyalakshmy, S. K. Halder, Cryst Eng Comm, **16**, 2802 (2014).
- [17] M. Senthil Pandian, K Boopathi, P Ramasamy, G Bhagavannarayana, Mater. Res. Bull. **47**, 826 (2012).
- [18] M. Senthil Pandian, Urit Charoen In, P. Ramasamy, Prapun Manyum, M. Lenin, N. Balamurugan, J. Cryst. Growth **312**, 397 (2010).
- [19] M. Senthil Pandian, P. Ramasamy, Binay Kumar, Mater. Res. Bull. **47**, 1587 (2012).
- [20] M. Senthil Pandian, P. Ramasamy, J. Cryst. Growth **312**, 413 (2010).
- [21] M. Senthil Pandian, P. Ramasamy, Mater. Chem. Phys. **132**, 1019 (2012).
- [22] B. Babu, J. Chandrasekaran, S. Balapabhakaran, Optik **125**, 3005 (2014).
- [23] M. Senthil Pandian, N. Balamurugan, V. Ganesh, P. V. Raja Shekar, K. Kishan Rao, P. Ramasamy, Mater. Lett. **62**, 3830 (2008).
- [24] M. Senthil Pandian, N. Pattanaboonmee, P. Ramasamy, P. Manyum, J. Cryst. Growth **314**, 207 (2011).
- [25] B. Babu, J. Chandrasekaran, S. Balapabhakaran, Mater. Sci-Poland **32**, 164 (2014).
- [26] S. K. Kurtz, T. T. Perry, J. Appl. Phys. **39**, 3798 (1968).

\*Corresponding author: jchandaravind@yahoo.com